Available online at www.sciencedirect.com
SCIENCE DIRECT®
Journal of Electroanalytical Chemistry 575 (2005) 19–26
Journal of Electroanalytical Chemistry
www.elsevier.com/locate/jelechem

Electrosynthesis and characterisation of poly(*N*-methylaniline) in organic solvents

Di Wei [a,b], Tom Lindfors [a,*], Carita Kvarnström [a], Leif Kronberg [c], Rainer Sjöholm [c], Ari Ivaska [a]

[a] *Process Chemistry Centre, c/o Laboratory of Analytical Chemistry, Åbo Akademi University, Biskopsgatan 8, Turku 20500 Åbo, Finland*
[b] *Graduate School of Materials Research (GSMR), Åbo Akademi University, Biskopsgatan 8, Turku 20500 Åbo, Finland*
[c] *Department of Organic Chemistry, Åbo Akademi University, Biskopsgatan 8, Turku 20500 Åbo, Finland*

Received 5 June 2004; received in revised form 23 August 2004; accepted 24 August 2004
Available online 26 October 2004

Abstract

The electropolymerisation of *N*-methylaniline was studied on glassy carbon and optically transparent tin oxide electrodes in the organic solvents dimethylformamide (DMF) and dimethyl sulfoxide (DMSO) containing 1.0 M methanesulfonic acid or 1.0 M trifluoromethanesulfonic acid. Our results show that a thin film of poly(*N*-methylaniline) can be obtained in DMF and DMSO, although the reaction product is very soluble. The PNMA film and the soluble fraction of the reaction product was analyzed and characterised with cyclic voltammetry, mass spectroscopy, in situ UV–Visible and Raman spectroscopy. The formation of an intermediate in DMF with an absorbance maximum at 720 nm was confirmed with in situ UV–Visible measurements. This is in contrast to polymerisation in aqueous solution where the absorbance maximum of the intermediate has been reported to appear at 441–460 nm.
© 2004 Elsevier B.V. All rights reserved.

Keywords: Conducting polymer; Electropolymerisation; Poly(*N*-methylaniline); Methanesulfonic acid; Trifluoromethanesulfonic acid; DMF; DMSO; Raman and UV–Visible spectroscopy

1. Introduction

Much less attention has so far been paid in the literature to *N*-substituted polyanilines than polyaniline (PANI) although there are several reports on both electrochemically and chemically synthesised poly(*N*-alkylanilines) [1–17]. They are interesting materials for several reasons. First, an intermediate with high stability is formed during electropolymerisation of various *N*-alkyl [8,11,12,14] or sulfoalkyl [10] substituted anilines in acidic aqueous solutions. It is therefore possible to perform both kinetic and mechanistic studies of the polymerization reaction of poly(*N*-alkylanilines) [12,14]. Second, the electrochemistry of poly(*N*-alkylanilines) is less complicated in comparison to PANI due to the absence of the very pH sensitive emeraldine base (EB)–emeraldine salt (ES) transition. It is generally agreed that the electrochemistry of poly(*N*-alkylanilines) in acidic solutions follows Scheme 1, where LE, E and PN denote the leucoemeraldine, emeraldine and pernigraniline forms of poly(*N*-methylaniline) (PNMA) [5,13]. It should be pointed out that the emeraldine form is the only electrically conducting form. Third, it has been reported that poly(*N*-methylaniline) is more stable towards oxidative degradation than PANI [6], although poly(*N*-benzylaniline) (PNBzA) was reported in another study to be less stable than PANI [12]. The higher stability of PNMA may eventually be a useful property in rechargeable battery applications [16].

* Corresponding author. Tel.: +358 2 215 4422; fax: +358 2 215 4479.
E-mail address: tom.lindfors@abo.fi (T. Lindfors).

0022-0728/$ - see front matter © 2004 Elsevier B.V. All rights reserved.
doi:10.1016/j.jelechem.2004.08.018

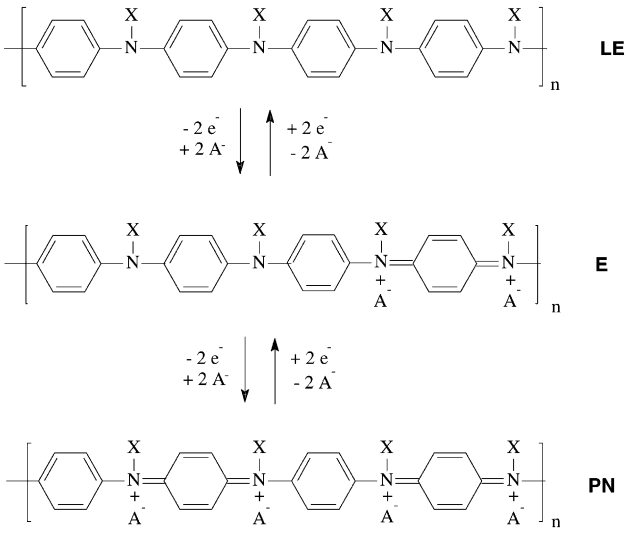

Scheme 1. The redox mechanism of PNMA prepared with a mobile counter anion (A^-). The leucoemeraldine, emeraldine and pernigraniline forms are indicated with LE, E and PN, respectively.

We recently reported that polymer films of PNMA, poly(*N*-ethylaniline) (PNEA), poly(*N*-propylaniline) (PNPA) and poly(*N*-butylaniline) (PNBA) can easily be formed on glassy carbon (GC) and tin oxide (TO) substrates in a 1.0 M $HClO_4$ solution [18]. It was also observed that the PNMA film growth was greatly facilitated in a 0.1 M solution of the surfactant dodecylbenzenesulfonic acid. The polymerisation of *N*-substituted anilines is usually done in acidic aqueous solutions, in order to avoid N–N coupling of the monomers [1], even though there are reports where *N*-heptylanilines and *N*-dodecylaniline were polymerised in acetonitrile (ACN) + H_2SO_4 [9] and ACN + $HClO_4$ mixtures [4], respectively. Chevalier et al. [4] have chemically synthesised different poly(*N*-alkylanilines) with different chain lengths (alkyl = methyl, ethyl, propyl, butyl, pentyl and dodecyl) and studied their solubility in different organic solvents. They showed that the polymers obtained were soluble in common organic solvents and therefore processable. The electrical conductivities of the poly(*N*-alkylanilines) were also reported to decrease with increasing chain length of the alkyl substituent. This was explained to be due to an increase in the interchain distance between adjacent polymer chains and an increase in the torsion angle between the phenyl rings, resulting in a decrease in the orbital overlap of the π-electrons.

It has recently been reported that the EB form of PANI contains between 5% and 15% water in its structure via hydrogen bonding [19]. This may possibly cause degradation of the polymer film upon oxidation. One possibility to avoid the presence of water in the polymer matrix is to perform the electropolymerisation in organic solvents. Osaka et al. [20–23] have studied the electropolymerisation of PANI in propylene carbonate (PC). They performed the electropolymerisation of PANI in a PC solution containing 0.5 M aniline, 0.5 M trifluoroacetic acid (CF_3COOH) and 0.5 M $LiClO_4$ as the electrolyte salt [21]. Miras et al. [24,25] have prepared electroactive PANI by anodic oxidation of non-protonated aniline in ACN. On the other hand, only one study concerning the electropolymerisation of *N*-substituted anilines in organic solvents has been reported to the best of our knowledge [17], i.e. the electropolymerisation of NMA in a PC solution containing 1 NMA, 4 CF_3COOH and 0.5 M $LiClO_4$. In the present paper, we have studied the electropolymerisation of NMA in the organic solvents dimethylformamide (DMF) and dimethyl sulfoxide (DMSO) containing 1.0 M methanesulfonic acid (MSA) or 1.0 M trifluoromethanesulfonic acid (FMSA). MSA and FMSA were chosen for this study because they are a medium strong and a strong acid, respectively, in both DMF and DMSO (MSA: $pK_a = 3.0$ in DMF; $pK_a = 1.6$ in DMSO) [26].

2. Experimental

2.1. Chemicals

N-methylaniline (NMA) (98.0%), methanesulfonic acid (MSA) (⩾99%) and dimethylformamide (DMF) (>99.8%) were obtained from Fluka and dimethyl sulfoxide (DMSO) (99.5%) from LabScan. All chemicals were used as received. Acetonitrile (ACN) from LabScan was freshly distilled and dried over basic alumina (≈150 mesh, Aldrich).

2.2. Cyclic voltammetry

The cyclic voltammetric (CV) measurements were performed in a three electrode cell with a GC disc (7 mm^2) as the working electrode (WE), a Pt wire as the counter electrode (CE) and a Ag|AgCl| 3 M KCl reference electrode (RE). The RE was placed in a bridge filled with 1.0 MSA or 1.0 M FMSA and the WE was polished mechanically with 0.3-μm alumina powder prior to all experiments. The electropolymerisation of NMA was done in DMF and DMSO containing 1.0 M MSA or 1.0 M FMSA. The PNMA films were characterised in monomer free solutions of 1.0 M MSA or 1.0 M FMSA in both DMF and DMSO, and the potential was controlled with an Autolab (PGSTAT 20) potentiostat. Prior to all measurements the solutions were purged with nitrogen and the solution were blanketed with nitrogen during the experiments.

2.3. Raman spectroscopy

In situ Raman spectra of the PNMA films were measured in a three electrode spectroelectrochemical cell that has been described elsewhere [27] (WE: GC (7 mm^2); CE: Pt wire; RE: Ag|AgCl wire calibrated vs ferroscene). The PNMA films were first characterised before the Raman measurements in an ACN solution containing 1.0 M MSA (1.0 M MSA–ACN). The spectra were then recorded at different potentials in the same solution by increasing the potential stepwise by 100 mV from 25 to 1025 mV. The 780 nm laser was focused on the PNMA film on a spot of ~10 μm in diameter and the scattering was collected at 90° with a Renishaw Raman imaging microscope (system 1000 B with a CCD detector).

2.4. UV–Visible spectroscopy

The UV–Visible transmission spectra were recorded with a Hitachi U-2001 spectrophotometer in a three electrode configuration in a standard 10 mm quartz cuvette. The electrode potential was first kept at 750 mV for 10 min and then at the open circuit potential for 10 min after the polymerisation. A quartz glass (thickness: 4 mm) coated with a thin layer of TO, a Pt and a Ag|AgCl wire served as WE, CE and RE, respectively. The TO glass was rinsed with acetone and an excess of deionised water prior to the measurements and the background spectra were always recorded with two blank TO glasses before the polymerisation was started. The measurements were done in a DMF solution containing 50, 100 or 500 mM NMA and 1.0 M MSA.

All experiments in this study were performed at 23 ± 1 °C.

2.5. Mass spectroscopy

The mass spectrometric (MS) analyses were performed with an Agilent 1100 Series LC/MSD SL Trap system (Agilent Technologies, Espoo/Esbo, Finland) equipped with an electrospray source and operated both in the positive and negative mode. Nitrogen was used as the nebulizer and drying gas (15 psi and 5 mL/min, respectively). The drying gas was heated to 325 °C and the capillary exit offset was adjusted to 128.5 V with skim 1 set at 40.0 V. The maximum ion accumulation time was 2000 μs and the target value was 30000. The full scan mass spectra were recorded by scanning from m/z 50–800. Helium was used as the collision gas in the collision induced dissociation experiments coupled with multiple tandem mass spectrometry (MS^n). The fragmentation amplitude was varied between 0.8 and 1.0 V and the samples with a concentration of ~5 μg/mL were introduced to the source by a syringe pump at a rate of 5 μL/min. A 1/1 mixture of 10 mM ammonium acetate + ACN was used as the solvent in the MS experiments.

3. Results and discussion

In general, electropolymerisation in organic solvents is influenced by various experimental parameters. First, the solvent will affect the chemical structure, conductivity, morphology and electrochemical behavior of the CP film. Second, the choice of the acid is crucial for the polymerisation process. A relatively strong proton donor, e.g. MSA and FMSA, resulting in a high proton activity in the organic solvent, is required in order to avoid N–N coupling of the monomer [1]. Third, the chemical structure and the thickness of the polymer film, which is formed during electropolymerisation, is affected by e.g. the monomer concentration and the upper switching potential.

In this work, the electropolymerisation of NMA was performed both in DMF and DMSO solutions containing 1.0 M MSA (hereafter abbreviated as 1.0 M MSA–DMF and 1.0 M MSA–DMSO, respectively) or 1.0 M FMSA (1.0 M FMSA–DMF and 1.0 M FMSA–DMSO). The effect of the monomer concentration (50, 100 and 500 mM) and the upper switching potentials (1025, 1050 and 1100 mV) was studied. The PNMA film formed on GC was studied with CV and in situ Raman spectroscopy and the soluble reaction product with in situ UV–Visible spectroscopy and MS.

3.1. Synthesis and characterisation of the PNMA film with CV

The polymerisation of 500 mM NMA in a 1.0 M MSA–DMF solution is shown in Fig. 1(a). A large amount of a highly soluble green coloured reaction product was formed in the vicinity of the WE soon after the polymerisation was started by cycling the potential between 25 and 1025 mV (50 cycles; scan rate: v = 50 mV/s). The soluble reaction product is formed in the 1.0 M MSA–DMF solution mainly at potentials higher than ~700 mV corresponding to the oxidation potential of NMA (Fig. 1(a), scan 1). The green reaction product, indicating the formation of the electrically conducting emeraldine form, separated continuously from the GC electrode and was dissolved in DMF during the electropolymerisation. A thin green film, however, covered the GC electrode after the polymerisation while no obvious film formation was observed on TO. Similar behaviour was found when the solvent was changed to DMSO or when the acid was changed to FMSA.

The influence of the monomer concentration (50, 100 and 500 mM) on the polymerisation of NMA in 1.0 M MSA–DMF was also studied. The film formation was slightly improved at the highest monomer concentration. The cross-over effect is rather strong at potentials higher than ~550 mV during the first 10 potential cycles, i.e. the current is higher during the negative scan in comparison to the positive scan (Fig. 1(a)). The high

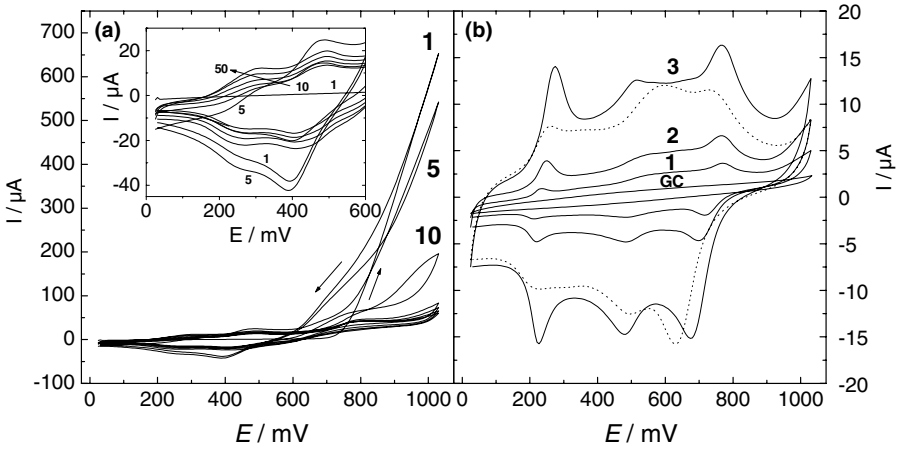

Fig. 1. (a) Polymerisation of 500 mM NMA in a 1.0 M MSA–DMF solution, v = 50 mV/s. The 1, 5, 10, 20, 30, 40 and 50th scans are shown in the figures and the potential interval of 25–600 mV is shown in the insert; (b) characterisation of the PNMA film in a 1.0 M MSA–DMF solution (2nd cycle: solid lines): (1) 10 mV/s, (2) 20 mV/s and (3) 50 mV/s. The CV of the bare GC electrode and the 20th cycle of the PNMA film (dotted line) are also shown in the figure, v = 50 mV/s.

monomer concentration (500 mM) facilitates the radical–radical coupling of the monomers and further oxidation of intermediate species formed at potentials higher than 550 mV contribute to the oxidative current that is observed during the negative scan. Dicationic species might also increase the number of coupling reactions leading to cross-linking between the intermediates. In general, a more cross-linked material is usually less soluble resulting in better adsorption of the reaction product at the electrode substrate. The upper switching potential (1025, 1050 and 1100 mV) did not have any significant influence on the doping response of the PNMA film in the potential range studied.

As can be seen in Fig. 1(b), three redox couples with $E_{pa,1} \cong 275$ mV/$E_{pc,1} = 226$ mV, $E_{pa,2} \cong 516$ mV/$E_{pc,2} = 480$ mV and $E_{pa,3} \cong 766$ mV/$E_{pc,3} = 676$ mV were observed when the PNMA film was characterised by CV in a 1.0 M MSA–DMF solution (v = 50 mV/s). The CVs recorded during the 2nd potential cycle at the scan rates of 10, 20 and 50 mV/s are shown in Fig. 1(b) (solid lines). The almost linear relationship between the anodic oxidation peak currents and the square root of scan rate indicates that the redox processes are controlled by diffusion of dopant anions (Scheme 1: A^-). Of the three redox couples in Fig. 1(b), the first couple at $E_{pa,1} \cong 275$ mV and the third couple at $E_{pa,3} \cong 766$ mV (v = 50 mV/s) can be ascribed to the LE–E and the E–PN transitions of PNMA (Scheme 1) [5]. As for PANI [28], the second redox couple at $E_{pa,2} \cong 516$ mV has been interpreted by Sivakumar and Saraswathi in an aqueous solution as associated with the hydroquinone–benzoquinone degradation product [17]. The anodic oxidation peak potentials of the PNMA film observed in this study are very similar to the peak potentials of PNMA obtained by Sivakumar and Saraswathi in an aqueous solution at pH 0. It should, however, be pointed out that all peak currents shown in Fig. 1(b) decrease after continuous cycling of the PNMA film in 1.0 M MSA–DMF in the potential interval of 25–1025 mV (see the 2nd (solid line) and 20th potential cycle (dotted line) of the PNMA film measured at v = 50 mV/s). The decreasing electroactivity of the PNMA film is probably caused by overoxidation in DMF, resulting in the formation of a degradation product, because the peak current of the second redox couple ($E_{pa,2} \cong 516$ mV) increases when the potential is cycled continuously to 1.1 V. At the same time, the peak currents of the first ($E_{pa,1} \cong 275$ mV) and third ($E_{pa,3} \cong 766$ mV) redox couples decrease.

The highest oxidation and reduction currents of the PNMA film were obtained when the electropolymerisation was performed in DMF with MSA. A PNMA film with lower currents was obtained when polymerizing in DMF with FMSA or in DMSO with MSA or FMSA.

3.2. Characterisation of the film by Raman spectroscopy

The electropolymerisation of the PNMA films for the Raman measurements was done in a 1.0 M MSA–DMF solution containing 500 mM NMA (see Section 3.1. and Fig. 1(a)). The PNMA films were, however, characterised with CV in 1.0 M MSA–ACN due to the strong interference of the Raman bands of DMF in the wavenumber interval studied (700–1850 cm^{-1}). The cyclic voltammogram of the PNMA film in ACN showing the three main redox couples at $E_{pa,1} = 479$, $E_{pa,2} \cong 580$ and $E_{pa,3} \cong 987$ mV differs significantly from the voltammogram of PNMA in DMF (Fig. 1(b)). For example, the oxidation and reduction peak currents for the third redox process at $E_{pa,3} \cong 987$ mV are much lower than for the first redox process at $E_{pa,1} = 479$ mV. The reason for this behaviour is still unclear at the moment.

The in situ Raman spectra were measured at the potentials (25–1025 mV) given in Fig. 2. The PNMA film was held for 2 min at each potential before the measurement was started and the laser light was applied to the sample. The Raman spectra measured at the different potentials are shown in Fig. 3 and have been separated from each other in order to clarify the spectral changes. It must, however, be stressed that the laser wavelength (λ_{exc} = 780 nm) used in this study will probably, due to resonance effects, enhance vibrations originating from the oxidised quinoid units, which are associated with the electrically conducting emeraldine form of PNMA [29] (Scheme 1).

The Raman bands in Fig. 3 at 762, 917 and 1369 cm^{-1} are characteristic of MSA and ACN (Table 1). These bands together with a band at ~1176 cm^{-1}, which is assigned to C–H in plane deformation (δ_{CH}) of the quinoid rings of the PNMA film [13], can mainly be observed in the spectra measured at potentials between 25 and 325 mV. The band at 1176 cm^{-1} is probably resonance enhanced by the laser used in this study. The broad band at 1595 cm^{-1} splits into two bands at 1616 and ~1587 cm^{-1} when the potential is increased to 425 mV. These two bands are assigned to the C–C and C=C stretching (ν_{CC}) of the benzenoid and quinoid rings, respectively [13,29]. Simultaneously, two new bands centered at ~1195 and ~1497 cm^{-1} appear in the spectra. The band at ~1195 cm^{-1} is assigned to C–H in plane deformation (δ_{CH}) of the benzenoid rings [13] and for PANI, the band at ~1497 cm^{-1} has been assigned to C=N stretching (ν_{CN}) of the quinoid rings [29]. The band at ~1497 cm^{-1}, which is associated with the electrically conducting emeraldine form of PNMA, indicates that the LE–E transformation (Scheme 1) starts approximately at 425 mV. This is in good accordance with the CV of PNMA in ACN showing that the LE–E transition starts at ~400 mV.

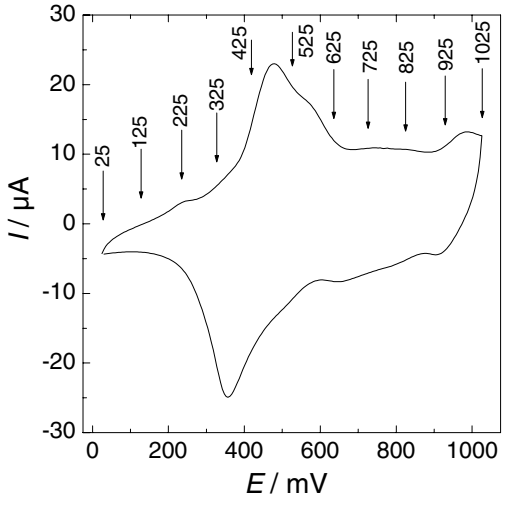

Fig. 2. Characterisation of the PNMA film in a 1.0 M MSA–ACN solution, v = 50 mV/s. The potentials that were applied in the Raman measurements are indicated with the arrows (see also Fig. 3).

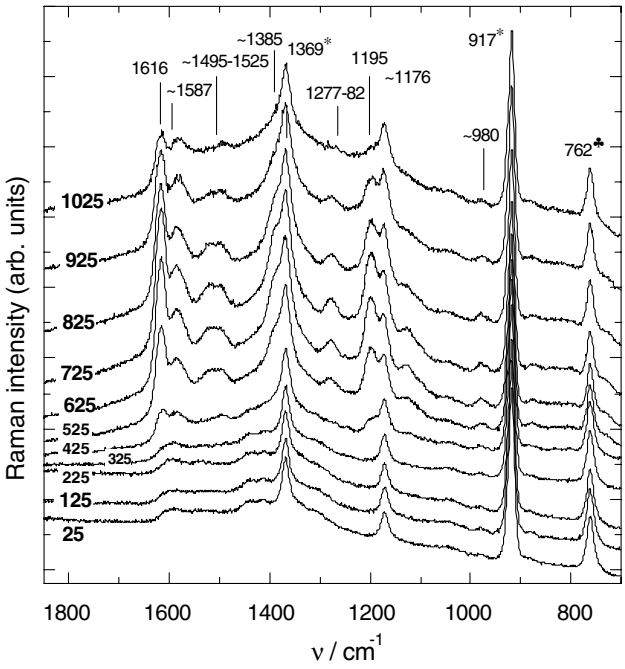

Fig. 3. The Raman spectra of PNMA in 1.0 MSA–ACN measured at different potentials (see also Fig. 2). The spectra were measured from 25 to 1025 mV. Peaks originating from ACN and MSA are indicated with * and ♣, respectively.

The strong growth of the benzenoid bands at ~1195 and 1616 cm^{-1} at potentials between 425 and 825 mV is somewhat contradictory because the amount of benzenoid units decreases in this potential range due to the conversion of benzenoid to quinoid units. Rather similar behavior was reported by Quillard et al. [29] when PANI was studied with the λ_{exc} = 676.4 nm laser in the potential interval of −150–600 mV (vs SCE).

A new band at ~1385 cm^{-1}, which is characteristic of C–N stretching (ν_{CN}) of the dicationic electrically conducting emeraldine form of PNMA [13], appears at potentials between 525 and 925 mV and overlaps partially with the ACN band at 1369 cm^{-1}. In this potential interval, the band at ~1497 cm^{-1} is transformed into a broad band centered at ~1510–1540 cm^{-1}. This is in good accordance with the results of Kilmartin and Wright [13]. Their Raman spectra of PNMA showed that the bands at 1374 and 1515 cm^{-1} were associated with the emeraldine form of PNMA. Simultaneously with the appearance of the band at ~1510–1540 cm^{-1}, a new band at ~1277–1282 cm^{-1} can also be observed in the spectra. This band is probably also related to the C–N stretching (ν_{CN}) of the dicationic semiquinone structure because it is expected that the modes involving the nitrogen atom will be most affected by direct substitution at the nitrogen atom [13]. At 925 mV the intensity of the bands at ~1277–1282, ~1385 and 1495–1525 cm^{-1} start to decrease indicating that the E–PN transition of

Table 1
Assignments of the main Raman bands shown in Fig. 3

Wavenumber (cm^{-1})		Assignment
762		MSA
917		ACN
~1176	Q	C—H in plane deformation (δ_{CH})
1195	B	C—H in plane deformation (δ_{CH})
1277–1282	E	C—N stretching (ν_{CN})
1369		ACN
~1385	E	C—N stretching (ν_{CN})
~1495–1525	E	C=N stretching (ν_{CN})
~1587	Q	C=C stretching (ν_{CC})
1616	B	C—C stretching (ν_{CC})

The benzenoid and quinoid units are denoted with B and Q, respectively. The electrically conducting emeraldine form of PNMA is indicated with E.

PNMA starts approximately at this potential, which is in good accordance with the CV of PNMA in ACN. The Raman spectra measured at 1025 mV show that the insulating PN form is the dominant form at this potential because almost no bands related to the E form of PNMA are present at ~1277–1282 and ~1385 cm^{-1}. A weak band can still, however, be observed at ~1495 cm^{-1} in the spectra measured at 1025 mV.

It can be concluded based on the CV and Raman measurements that a thin PNMA film can be formed in a 1.0 M MSA–DMF solution. The potential dependent changes observed in the Raman spectra and the CV of PNMA in ACN are in good accordance with each other, confirming that the LE–E and E–PN transitions take place in the PNMA film.

3.3. Characterisation of the soluble fraction of the reaction product

The soluble part of the reaction product formed during the electropolymerisation of 50, 100 and 500 mM NMA in 1.0 M MSA–DMF was studied with UV–Visible spectroscopy. The UV–Visible spectra that were recorded every minute at 750 mV are shown as solid lines in Fig. 4 and the spectra taken at the open circuit potential (E_{ocp}) as dotted lines. Three absorbance maxima can be distinguished in the spectra at 405, 720 and 1005 nm. The maxima at 405 and 1005 nm are characteristic of the electrically conducting emeraldine form [1,4]. The absorbance maxima of these bands are almost proportional to the NMA concentration while the absorbance maximum of the band at 720 nm is not proportional to the NMA concentration. When the potential is switched to the open circuit potential after performing the polymerisation for 10 min at 750 mV, the band at 720 nm disappears almost completely in contrast to the bands at 405 and 1005 nm, which decrease in intensity only to a minor extent (Figs. 4 and 5). It should be noted that the absorbance, especially at 1005 nm, still increases for 1–2 min after the polymerisation is completed, which is typical for a coupled chemical reaction. This could, however, also be due to accumulation of the reaction product in the light path of the photometer after switching the potential to the open circuit potential at $t = 10$ min. The strong decrease of the absorbance maximum at 720 nm is obviously related to an intermediate that reacts further, forming an end product, which is observed at 405 and 1005 nm. The spectra recorded after 20 min are very similar to the spectra of the emeraldine form of the PNMA film in aqueous solution [4,30]. The formation of the end product is favoured at higher NMA concentrations because more intermediate is formed with a higher probability to react with the excess of NMA. No reaction products could, however, be identified with MS analysis when the polymerisation was performed in 1.0 M MSA–DMF with 500 mM NMA, even though it was visually observed that great amounts of a green coloured reaction

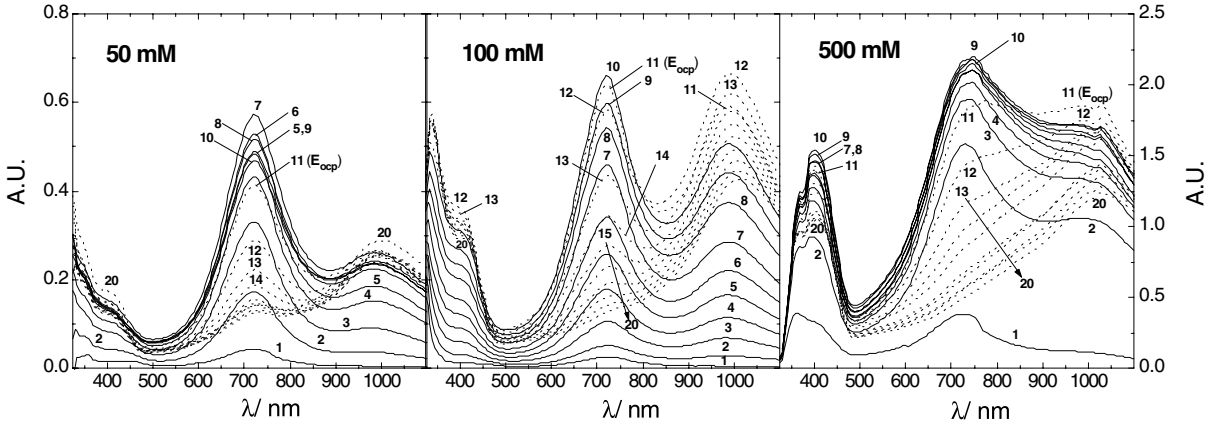

Fig. 4. The UV–Visible spectra recorded during polymerisation of 50, 100 and 500 mM NMA at 750 mV in a 1.0 M MSA–DMF solution. One spectrum was recorded every minute for 20 min as indicated by the numbers in the figures. The spectra were first recorded for 10 min at 750 mV (solid lines) and then 10 min at the open circuit potential, E_{ocp} (dotted lines). The scale of the absorbance axes in the figures showing the polymerisation of

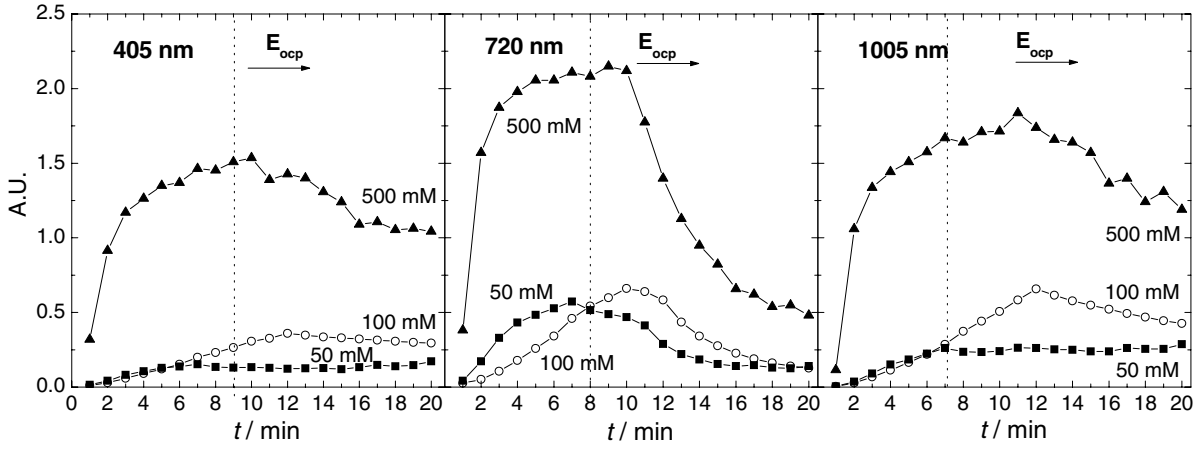

Fig. 5. The absorbance vs time at 405, 720 and 1005 nm measured during polymerisation of 50, 100 and 500 mM NMA at 750 mV in a 1.0 M MSA–DMF solution (see Fig. 4). The potential was first held for 10 min at 750 mV and then 10 min at the open circuit potential (E_{ocp}).

product were formed in the vicinity of the WE, changing the colour of the polymerisation solution from transparent to dark green. The green coloured reaction product has a very weak affinity to the TO surface and no growth of the PNMA film on the TO electrode was observed. It should therefore be pointed out that the absorbance bands at 405, 720 and 1005 nm arise from solution species only. The MS measurements indicate, however, that trimers or tetramers are formed when the polymerisation of NMA is performed in 1.0 M FMSA–DMF.

It has been shown by Malinauskas and Holze [18] that *N*-substituted anilines form very stable intermediates that can be detected on a minute time scale with in situ UV–Visible spectroscopy. They also confirmed that the electropolymerisation of NMA follows an EC mechanism. It was, however, reported that the intermediate formed in the electropolymerisation of NMA, *N*-ethylaniline (NEA), *N*-benzylaniline (NBzA) and *N*-(3-sulfopropyl)aniline (NSPA) in acidic aqueous solution has an absorbance maximum at 441 nm [14], 443 nm [8] (NMA), 450 nm [11] (NEA), 453 nm [10] (NSPA) and 460 nm [12] (NBzA). The differences in the absorbance maxima of the intermediate in aqueous solution and DMF may be caused by a different polymerisation mechanism of NMA in DMF than in aqueous solution or by differences in the chemical and physical properties, e.g. polarity, of these two solvents. In the case of NSPA, it was proposed that nitrenium cation intermediates were formed although this could not be verified chemically [10].

4. Conclusions

Thin films of PNMA can be electropolymerised on GC in the organic solvent DMF containing the moderately strong acid MSA. The PNMA films that were characterised with CV and in situ Raman spectroscopy showed the characteristic LE–E and E–PN transitions typical for PNMA in acidic aqueous solution. Most of the reaction product is, however, soluble in DMF and does not undergo further polymerisation and precipitation on the electrode. Analysis of the soluble fraction of the reaction product with in situ UV–Visible spectroscopy showed that a very stable intermediate is formed with an absorbance maximum at 720 nm. This intermediate, which reacts further to an end product, is usually observed at 441–460 nm in aqueous solutions. The difference in the absorbance maximum of the intermediate in aqueous solution and DMF may be due to a different polymerization mechanism of NMA in DMF or differences in the chemical and physical properties, e.g. polarity, of DMF and water.

PNMA films prepared in organic solvents may possibly be used as inner ion-to-electron transducer layers in all-solid-state ion-selective electrodes. The main advantages are that these layers can be prepared without the presence of water and that they are pH insensitive in contrast to PANI [31]. Water will accumulate in the ion-to-electron transducer layer when the electropolymerisation is performed in aqueous solution. This is expected to induce long-term instability of this layer.

Acknowledgement

This work is part of the activities of the Åbo Akademi Process Chemistry Centre within the Finnish Centre of Excellence Programme (2000–2005) sponsored by the Academy of Finland.

References

[1] N. Comisso, S. Daolio, G. Mengoli, R. Salmaso, S. Zecchin, G. Zotti, J. Electroanal. Chem. 255 (1988) 97.

[2] J.W. Chevalier, J.Y. Bergeron, L.H. Dao, Polym. Commun. 30 (1989) 308.
[3] A. Watanabe, K. Mori, A. Iwabuchi, Y. Iwasaki, Y. Nakamura, O. Ito, Macromolecules 22 (1989) 3521.
[4] J.W. Chevalier, J.Y. Bergeron, L.H. Dao, Macromolecules 25 (1992) 3325.
[5] C. Barbero, M.C. Miras, O. Haas, R. Kötz, J. Electroanal. Chem. 310 (1991) 437.
[6] J. Yano, M. Kokura, K. Ogura, J. Appl. Electrochem. 24 (1994) 1164.
[7] A. Lian, S. Besner, L.H. Dao, Synth. Met. 74 (1995) 21.
[8] A. Malinauskas, R. Holze, Ber. Bunsenges. Phys. Chem. 101 (1997) 1859.
[9] A. Kitani, H. Munemura, Y. Ota, K. Takaki, S. Ito, Mol. Cryst. Liq. Cryst. 296 (1997) 349.
[10] A. Malinauskas, R. Holze, Electrochim. Acta 43 (1998) 2413.
[11] A. Malinauskas, R. Holze, Electrochim. Acta 44 (1999) 2613.
[12] A. Malinauskas, R. Holze, J. Solid State Electrochem. 3 (1999) 429.
[13] P.A. Kilmartin, G.A. Wright, Synth. Met. 104 (1999) 145.
[14] C. Sivakumar, A. Gopalan, T. Vasudevan, T.-C. Wen, Synth. Met. 126 (2002) 123.
[15] G.A. Planes, M.C. Miras, C. Barbero, Polym. Int. 51 (2002) 429.
[16] R. Sivakumar, R. Saraswathi, J. Power Sources 104 (2002) 226.
[17] R. Sivakumar, R. Saraswathi, Synth. Met. 138 (2003) 381.
[18] T. Lindfors, A. Ivaska, J. Electroanal. Chem. 535 (2002) 65.
[19] W. Łużny, M. Śniechowski, Fibers Text. East. Eur. 11 (2003) 75.
[20] T. Osaka, S. Ogano, K. Naoi, J. Electrochem. Soc. 135 (1988) 539.
[21] T. Osaka, S. Ogano, K. Naoi, N. Oyama, J. Electrochem. Soc. 136 (1989) 306.
[22] T. Osaka, T. Nakajima, K. Naoi, B.B. Owens, J. Electrochem. Soc. 137 (1990) 2139.
[23] T. Osaka, T. Nakajima, K. Shiota, T. Momma, J. Electrochem. Soc. 138 (1991) 2853.
[24] M.C. Miras, C. Barbero, O. Haas, Synth. Met. 43 (1991) 3081.
[25] M.C. Miras, C. Barbero, R. Kotz, O. Haas, J. Electrochem. Soc. 138 (1991) 335.
[26] K. Izutsu, Electrochemistry in Non-aqueous Solvents, Wiley, Weinheim, 2002, pp. 66–67.
[27] P. Damlin, C. Kvarnström, A. Petr, P. Ek, L. Dunsch, A. Ivaska, J. Solid State Electrochem. 6 (2002) 291.
[28] L.D. Arsov, W. Plieth, G. Kossmehl, J. Solid State Electrochem. 2 (1998) 355.
[29] S. Quillard, K. Berrada, G. Louarn, S. Lefrant, M. Lapkowski, A. Pron, New J. Chem. 19 (1995) 365.
[30] T. Lindfors, A. Ivaska, J. Electroanal. Chem. 531 (2002) 43.
[31] T. Lindfors, A. Ivaska, Anal. Chem. 76 (2004) 4387.